Int. J. Radiation Oncology Biol. Phys., Vol. 76, No. 4, pp. 1266–1273, 2010

0360-3016/10/$–see front matter

ELSEVIER

doi:10.1016/j.ijrobp.2009.07.1686

PHYSICS CONTRIBUTION

DYNAMIC JAWS AND DYNAMIC COUCH IN HELICAL TOMOTHERAPY

Florian Sterzing, M.D.,* Matthias Uhl, M.D.,* Henrik Hauswald, M.D.,* Kai Schubert, Ph.D.,* Gabriele Sroka-Perez, Ph.D.,* Yu Chen, Ph.D.,† Weiguo Lu, Ph.D.,† Rock Mackie, Ph.D.,† Jürgen Debus, M.D., Ph.D.,* Klaus Herfarth, M.D.,* and Gustavo Oliveira, Ph.D.†

*Department of Radiation Oncology, University of Heidelberg, Germany; and †Tomotherapy Incorporated, Madison, Wisconsin

Purpose: To investigate the next generation of helical tomotherapy delivery with dynamic jaw and dynamic couch movements.

Methods and Materials: The new technique of dynamic jaw and dynamic couch movements is described, and a comparative planning study is performed. Ten nasopharyngeal cancer patients with skull base infiltration were chosen for this comparison of longitudinal dose profiles using regular tomotherapy delivery, running-start-stop treatment, and dynamic jaw and dynamic couch delivery. A multifocal simultaneous integrated boost concept was used (70.4Gy to the primary tumor and involved lymph nodes; 57.4Gy to the bilateral cervical lymphatic drainage pathways, 32 fractions). Target coverage, conformity, homogeneity, sparing of organs at risk, integral dose, and radiation delivery time were evaluated.

Results: Mean parotid dose for all different deliveries was between 24.8 and 26.1Gy, without significant differences. The mean integral dose was lowered by 6.3% by using the dynamic technique, in comparison with a 2.5-cm-field width for regular delivery and 16.7% with 5-cm-field width for regular delivery. Dynamic jaw and couch movements reduced the calculated radiation time by 66% of the time required with regular 2.5-cm-field width delivery (199 sec vs. 595 sec, $p < 0.001$).

Conclusions: The current delivery mode of helical tomotherapy produces dose distributions with conformal avoidance of parotid glands, brain stem, and spinal cord. The new technology with dynamic jaw and couch movements improves the plan quality by reducing the dose penumbra and thereby reducing the integral dose. In addition, radiation time is reduced by 66% of the regular delivery time. © 2010 Elsevier Inc.

Helical tomotherapy, Dynamic jaws, Dynamic couch, Longitudinal dose profile, Nasopharyngeal cancer.

INTRODUCTION

Helical tomotherapy is a unique solution of image-guided intensity-modulated radiotherapy (IMRT) that has been in clinical use for approximately 5 years. Its physical characteristics of megavoltage imaging and helical beam delivery have been described previously (1–3). The capabilities of producing conformal dose distributions in various oncological situations have been shown in numerous publications (4). A special characteristic of the system is the possibility of treating the most challenging cases in radiation oncology in terms of size, complex geometry, and difficulty in sparing of normal tissue (5–9).

For head and neck cancer patients, excellent sparing of parotid glands and pharyngeal constrictors has been reported, allowing xerostomia and dysphagia to be minimized (10–12). This is of extraordinary importance to the quality of life of the patients, particularly for patient groups characterized by high cure rates, *e.g.*, nasopharyngeal cancer patients (13, 14).

Although the one outstanding feature of helical tomotherapy is dynamic movement, there is some limitation to this feature. Once certain parameters for couch and gantry movements are chosen during the planning process, they will be constant throughout the entire treatment (pitch, field width, couch speed). For many clinical situations, a reasonable combination of these parameters will produce fine quality plans. However, some longer target volumes with different areas of complexity and proximity of organs at risk are forced to be treated with a compromise solution. This is especially true for the treatment

Reprint requests to: Florian Sterzing, M.D., Department of Radiation Oncology, University of Heidelberg, INF 400, 69120 Heidelberg, Germany. Tel: (0049) 6221-568202; Fax: (0049) 6221-565353; E-mail: florian.sterzing@med.uni-heidelberg.de

This work was supported by TomoTherapy Incorporated, Madison, WI, within a research collaboration, and by the Deutsche Krebshilfe and the German Research Foundation (DFG).

Conflict of interest: WF, YC, RM, and GO are employees of Tomotherapy Inc. Madison, WI. FS, MU, HH, KS, GSP, JD, and KH receive research funding from Tomotherapy Inc. Madison, WI, within a research collaboration.

Acknowledgment—We dedicate this article to our friend and colleague Sam Jeswani, with gratitude for his professional inspiration and matchless friendship.

Received April 9, 2009, and in revised form July 8, 2009. Accepted for publication July 9, 2009.

of targets where the ''travel distance'' between target volumes is covered without any option to move faster. The dose application during patient movement causes a phenomenon of dose spillage superiorly and inferiorly to the target. Radiation starts when the inferior edge of the fan beam is entered by the superior border of the target volume. Therefore, a dose penumbra with a dimension defined by the chosen field width is produced. This phenomenon can be problematic when sharp craniocaudal dose gradients are needed, making the use of a bigger fan beam width unsuitable (4, 15).

The idea of adding even more dynamic components to helical tomotherapy with dynamic jaw and dynamic couch (DJDC) movements was already included in the first publication on tomotherapy in 1993 (16). With this technology, the jaws are not static during the treatment, they are moving to track the exact border of the target volume, and they can be flexibly adapted to different areas of a target (17). In addition, the couch movement can change during treatment, accelerating the fraction time by skipping travel distance between targets or by simply moving faster in areas that do not require a huge amount of intensity modulation.

The present work describes the different components and combinations of DJDC movements in helical tomotherapy. We present the first study of radiation plans acquired with a new prototype software that compares dose distributions in regular and dynamic tomotherapy delivery. Nasopharyngeal cancer patients with skull base involvement were chosen for this comparative planning study, since sharp longitudinal dose gradients necessary to spare the optic pathways and brain tissue are most evident here.

METHODS AND MATERIALS

Patients

Ten patients with locally advanced nasopharyngeal cancer were chosen for this planning study. Tumor stages were T4N2M0 (n = 6 patients), T4N1M0 (n = 2 patients), T3N2M0 (n = 1 patient), and T3N1M0 (n = 1 patient). The mean size of the primary tumor planning tumor volume (PTV) was 176 cm^3, the lymph node metastases boost PTV was 67 cm^3, and the nodal PTV was 852 cm^3.

The minimal average distance to the optic pathway was 2.4 mm for the boost PTV and 4.2 mm for the nodal PTV. The average length of the target volume was 20.1 cm (range, 16.2 cm–24 cm).

Radiotherapy planning

Tomotherapy planning was based upon a computed tomography (CT) scan with 3-mm-slice thickness that included the skull base down to the tracheal bifurcation. A three-dimensional fusion with either contrast-enhanced magnetic resonance imaging (MRI) or [^{18}F]fluoro-2-deoxyglucose positron emission tomography (FDG-PET) was performed for target volume definition.

Target volumes and dose prescription

Simultaneous multifocal integrated boost plans were created with three different target volumes, as follows.

Primary tumor boost. Gross tumor volume (GTV) included the tumor extension as detected on contrast-enhanced MRI or FDG-PET. Clinical tumor volume (CTV) consisted of the GTV expanded by a 5- to 10-mm margin, depending on the specific area, including the nasopharyngeal cavity, base of skull, posterior nasal cavity, pterygoid fossae, clivus, and sphenoid sinus. The PTV consisted of the CTV expanded by an additional 3 mm. All expansions excluded structures at risk, like spinal cord, brain stem, or optic pathways. Median prescription dose was 70.4 Gy in 32 fractions to the PTV.

Involved lymph node boost. GTV encompassed pathological nodes greater than 1 cm. CTV included GTV expansion by 5 mm. PTV included CTV expansion of 3 mm. The median prescription dose was 70.4 Gy in 32 fractions to the PTV.

Lymphatic drainage. CTV included bilateral cervical lymph nodes at levels Ib to V (12, 13, 18, 19), encompassing the medial supraclavicular fossae and parts of the medial lobe of parotid glands to avoid local recurrence in spared periparotid areas (20). PTV consisted of the CTV expanded by 3 mm, not exceeding the skin level. A median dose of 57.4 Gy in 32 fractions was prescribed.

Organs at risk

Relevant organs at risk and dose constraints for planning are listed in Table 1. Additional volumes of interest included skin contour to evaluate integral dose, a concentric structure with a 2.5-cm margin around the nodal PTV to optimize conformity, a structure in the neck to avoid hot spots below the spinal cord, and a tuning volume of interest (VOI) in the jugular area to avoid hot spots of the skin.

Dynamic tomotherapy delivery

In addition to the characteristic moving features of present tomotherapy delivery (gantry, collimator, and couch), the new dynamic tomotherapy delivery introduces flexibility of two components: the jaws and the couch. It enables different combinations of dynamic components displayed in Table 2.

Using independent jaw motions, the running-start-stop (RSS) delivery refers to the flexible adoption of front (inferior) and back (superior) field borders to the edges of the target volume. Irradiation starts at the moment the superior edge of the tumor enters the field projected by the open inferior (front) jaw. The back jaw then follows the tumor edge with the speed of the couch until the opening width of the jaw is reached. While the tumor is moved through the fan beam, the jaw position and, consequently, the field width remain constant. At the distal end of the target volume, a process that mirrors that in the beginning happens with the tracking of the inferior edge of the target volume. Figure 1 displays the difference between dynamic jaw movement and regular tomotherapy delivery. The organ at risk directly above the tumor is exposed to the dose in regular delivery, while this dose penumbra is cut off by the individual movement of the upper jaw in RSS delivery.

In addition, the field width can also be changed within the target volume. This is referred to as dynamic jaws, and it can facilitate a customized handling of different areas of a tumor that require more or less precision. The jaw width and the couch motion are determined based on the longitudinal fluence profile. Then, the leaf-open times are optimized, given the jaw and couch trajectories. By allowing the couch to travel at different speeds, this customized adaptation can even be intensified so that the combination of DJDC will offer the highest degree of dynamic flexibility. In addition, distances between separated lesions can be covered with a speed of up to 10 cm/sec, leading to a further reduction of treatment time.

The fluence irradiating a voxel is inversely proportional to the couch speed. The ability to modulate the couch velocity depends on the maximum couch acceleration allowed, which during treatment, should be less than the limit of perceptibility of acceleration. If 1% of the acceleration due to gravity is the limit on acceleration and the couch speed must be changed to 5 mm/sec from 1 mm/sec in order

Table 1. Planning objectives for relevant organs at risk

Organ	Mean dose	Maximum dose
Brain	As low as possible	
Brainstem	As low as possible	<54 Gy
Spinal cord		<45 Gy
Eyes		<20 Gy
Lenses	<3 Gy	
Optic nerves plus chiasm		<54 Gy
Parotids	<26 Gy	
Inner ears	<40 Gy	<54 Gy
Temporomandibular joints	<40 Gy	
Oral cavity	As low as possible	
Lips	As low as possible	
Larynx and pharyngeal constrictors	<40 Gy	<50 Gy
Esophagus	<30 Gy	<50 Gy
Pulmonary apex	As low as possible	

to lower the intensity to 20%, this can be done in less than half a second, which is on the order of the time interval required for one cycle of opening and closing of the multileaf collimator (MLC). Humans can also detect surge, which is a change in acceleration. As shown in Fig. 2, this means that couch modulation can closely track the required fluence rate but is dampened to make the surge imperceptible.

The dynamic jaw techniques including RSS improve longitudinal conformity by allowing a much smaller jaw width near the superior and inferior borders of the target. Furthermore, the DJDC combination maximizes the jaw width and, consequently, the beam utilization, which improves efficiency and thus reduces beam-on time. The intensity modulation along the longitudinal direction is accounted for by varying the couch speed. A variable couch speed allows different patient slices to stay in the radiation beam for a different amount of time. Leaf-open time was the only way to implement such a variation when only jaw width and constant couch speed could be chosen for a plan. Therefore, DJDC techniques can reduce the modulation factor used for leaf-open optimization, which further improves the efficiency and reduces beam-on time.

Tomotherapy planning

Regular tomotherapy planning was done with the tomotherapy planning station version 3.1.2.9. Two plans with field widths of 2.5 cm and 5 cm (REG 2.5 and REG 5) were created. Although the 5-cm-field width was not considered clinically suitable due to the dose penumbra, it was planned to quantify the differences between regular and dynamic delivery. A pitch of 0.287 was chosen to reduce thread effect (21). Optimization was started with an intensity modulation factor (IMF) of 2.0; toward the end of planning, it was increased to 3.5.

Inverse planning for dynamic tomotherapy delivery was performed with the research planning station version 6.1.0.10. For each patient, an RSS plan with maximum field widths of 2.5 cm and 5 cm (RSS 2.5 and RSS 5) was created. In addition, a DJDC plan for a maximal field width of 5 cm (DJDC 5) is presented. A pitch of 0.287 was used. The IMF was 2.0 at the beginning of RSS planning and was increased toward the end of optimization to 3.5. In DJDC planning, the IMF was first set to 3.5 and later on slowly decreased to a level of 1.8–2.2 to accelerate couch movement.

Plan evaluation

The uniformity index (UI) is calculated as the ratio between the dose (D) received by 5% of the PTV and the dose received by 95% of the PTV, *i.e.*, UI = $D_{5\%}/D_{95\%}$. In addition, the conformity index (CI) is calculated as the ratio between the volume enclosed by the 95% isodose volume and the part of the target receiving more than 95%, *i.e.*, $CI_{95\%} = V_{95\%}/TV_{95\%}$.

The integral dose is calculated as the product of tissue volume and mean tissue dose (22). Calculations of statistical significance were performed with the two-sided Student's *t* test. A *p* value of <0.05 was considered statistically significant.

RESULTS

With the current delivery mode of helical tomotherapy, all dose constraints for the organs at risk are reached together with excellent target coverage and conformity. The RSS mode is able to produce sharp dose gradients with improved longitudinal dose conformity. The DJDC movement produces the same dose gradients with a time reduction of 67% (DJDC 5 vs. REG 2.5). Figure 3 shows the dose distributions for the different delivery modes, and Table 3 lists dosimetric characteristics of the plans as average values.

Regular tomotherapy delivery with differing fixed jaw widths

A comparison of the plans of the currently available delivery mode for tomotherapy with 2.5-cm- and 5-cm-field widths shows the consequences of an increased superior and inferior dose penumbra. This causes increased volumes of brain, optic pathways, and lung tissue to be exposed to dose and forces acceptance of underdosing the boost to maintain tolerance dose levels ($TV_{95\%}$ boost 95% in REG 2.5 vs. 88.2% in REG 5, $p = 0.003$). The mean radiation time is reduced by 47% with the use of a 5-cm-jaw width instead of a 2.5-cm width, but the integral dose is increased by 12.5% ($p < 0.001$ and $p = 0.02$, respectively). Clinically, a regular delivery with a 5-cm-jaw opening in a complex volume such as this would not be acceptable.

Regular vs. RSS delivery

In contrast to the regular delivery mode, RSS technology enables the use of the 5-cm-field width due to the avoidance of the dose penumbra. Therefore, the coverage can be improved with a $TV_{95\%}$ boost of 95% in REG 2.5 vs. 96.6% in RSS 5 ($p = 0.03$). The integral dose is reduced by 5.7%

Table 2. Combinations of dynamic components in the new delivery mode

Mode	Jaws	Couch
Regular	Constant	Constant
Running-start-stop	Adjustable beginning and end Constant in between	Constant
Dynamic jaw and constant couch	Dynamic everywhere	Constant
Dynamic symmetric jaw dynamic couch	Symmetric but dynamic	Dynamic
Dynamic jaw and dynamic couch	Dynamic	Dynamic

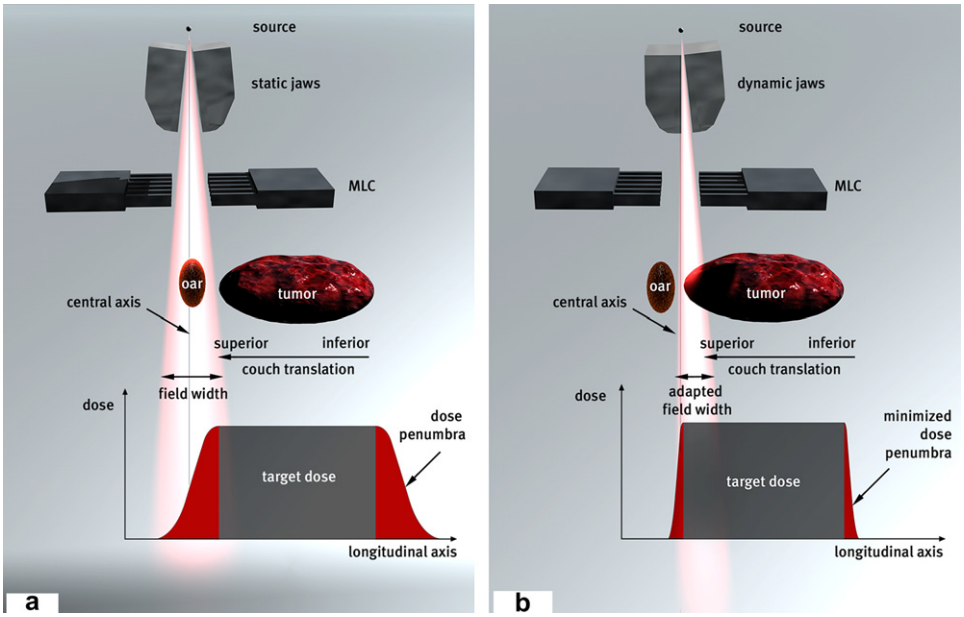

Fig. 1. Outline of jaw and fan beam characteristics of different delivery modes: (a) regular tomotherapy delivery causes a considerable dose penumbra above and below the target, whereas (b) RSS delivery with dynamic jaws reduces this dose exposure to healthy tissue. oar = organ at risk.

with the new technology ($p = 0.02$). Calculated radiation time is reduced by 44% ($p < 0.001$).

Regular vs. DJDC delivery

The DJDC mode enables dosimetric characteristics similar to the RSS mode but can accelerate the delivery even more (an extra 40% in time gain).

Since regular delivery with 2.5-cm jaws offers the best currently available clinical compromise between radiation time and dose conformity, the comparison between REG 2.5 and DJDC 5 is the most interesting from a practical standpoint. Using DJDC delivery, the calculated radiation time is reduced by 66% of the time required with regular delivery using 2.5-cm-field width (199 sec vs. 595 sec, $p < 0.001$). The mean integral dose is lowered by 6.3%, using the DJDC mode ($p = 0.0003$). The boost conformity decreased from a $CI_{95\%}$ of 1.11 to 1.34 ($p < 0.001$). The average optic nerve dose is decreased from 34.5 Gy to 28 Gy, and the average chiasm dose decreased from 39.5 Gy to 21.3 Gy (both, $p < 0.001$). At the same time, the maximum dose to the optic nerves is decreased from 50.9 to 46.9 Gy, and dose to the chiasm is decreased from 49.1 to 31.8 Gy (both, $p < 0.001$).

Comparing the currently fastest mode (REG 5) and the fastest future option (DJDC 5), the integral dose is lowered by 16.6% ($p < 0.001$), and radiation time is reduced by 38% ($p < 0.001$).

Mean parotid dose for all different deliveries was between 24.8 and 26.1 Gy, without significant differences. Brain stem and spinal cord doses were within tolerance levels and without statistical differences. Average doses to larynx and pharyngeal constrictors were between 33.4 and 37.8 Gy in the different delivery modes, also without significant changes.

DISCUSSION

This is the first work that presents plans and dose distributions of the next generation delivery mode of helical tomotherapy with DJDC motion. This technique promises to be a great step forward in terms of improved plan quality for the patient and reduced time to deliver the treatment dose.

The possibilities of helical tomotherapy for nasopharyngeal cancer treatment with a simultaneous integrated boost concept have been shown previously (11, 14). However,

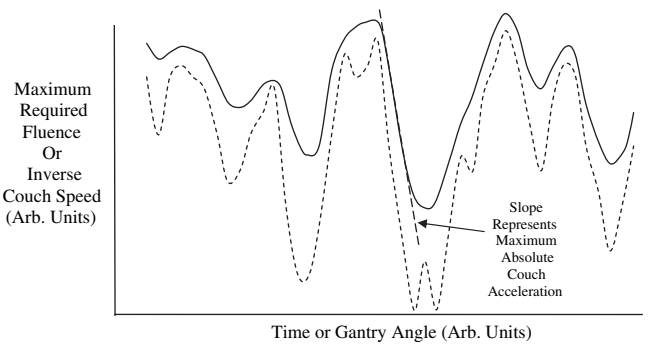

Fig. 2. The maximum required fluence rate (dashed line) is the maximum rate of fluence required for any given projection, where one projection is one cycle of opening and closing of the MLC. The fluence directed toward a voxel is proportional to the integral of the inverse of the instantaneous couch speed times the maximum fluence rate during the projections times the relative opening times for all projections irradiating that voxel. The inverse couch speed (solid line) can be modulated to reduce the requirements of the fluence modulation by the MLC. This allows more efficient use of MLC modulation. The major constraint of the couch to provide modulation depends on the maximum acceleration allowed. The maximum acceleration (straight dashed line) should be no more than a few percentage points of the gravitational acceleration in order for the couch velocity modulation to be imperceptible to the patient.

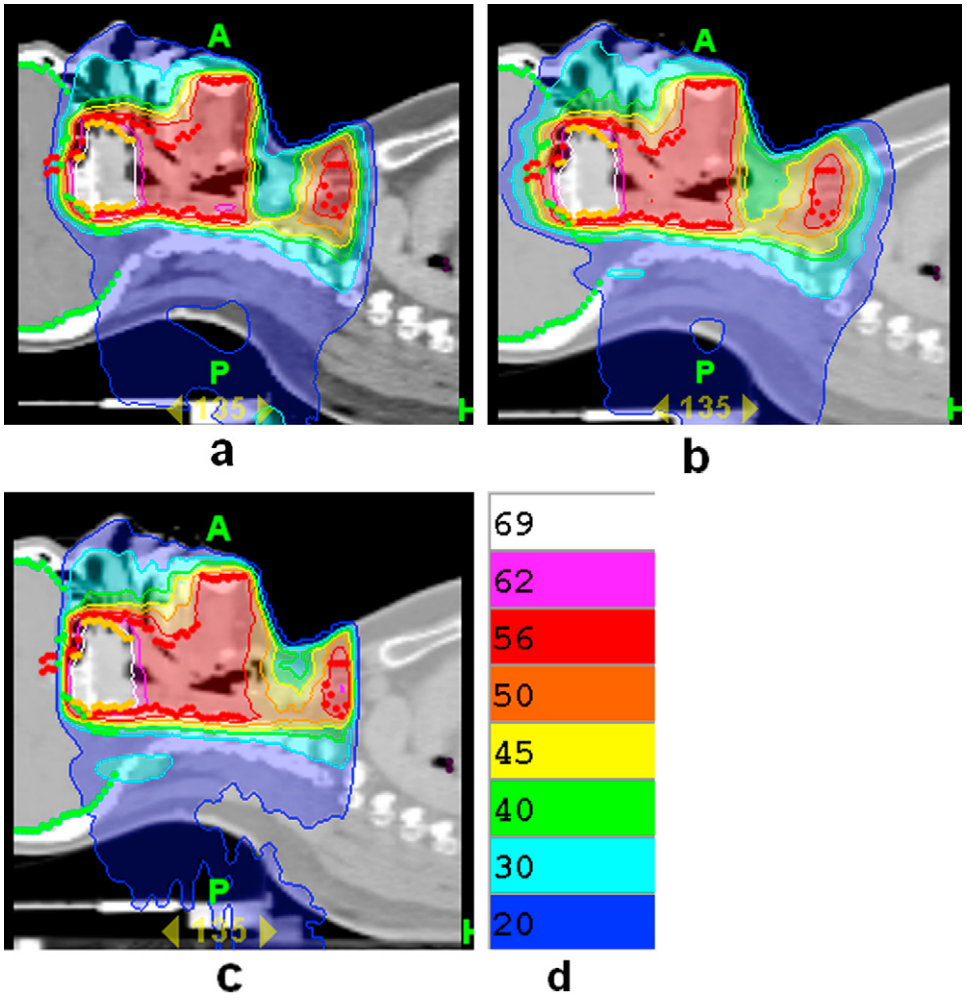

Fig. 3. (a–d) Dose distribution for one patient of regular delivery with 2.5-cm-field width (REG 2.5) and 5-cm-field width (REG 5) and DJDC delivery with 5 cm (DJDC 5), doses are shown in Gy.

this study presents treatment results for a group of nasopharyngeal cancer patients with advanced cases of skull base infiltration and very short distances to the optic pathways and brainstem. Since these patients had advanced disease in both the primary tumor and within the lymph nodes, we chose an aggressive high-dose regimen for all target volumes. Even in this constellation of advanced diseases in problematic localizations and high therapeutic doses, we were able to create plans of excellent dose coverage and conformity with a sparing of organs at risk that met all planning constraints. The mean parotid dose of 24.8 Gy and the dose reduction to the pharyngeal constrictors of 34.3 Gy are of great importance to the quality of life of our patients (23). The UI with a mean of 1.18 in the nodal PTV is not very close to 1 because of the integrated boost concept that is purposely producing nonuniform dose escalation within the target area. The plans with a field width of 2.5 cm seem to be the optimal solution for clinical treatment in regular delivery mode with the best compromise between speed and dose distribution. The 5-cm regular plan compared to the 2.5-cm regular plan saves a lot of time, but the 5-cm-dose penumbra and the dose exposure both to the brain and to the lungs do not make it suitable for clinical application for this particular patient group.

The next generation of tomotherapy with dynamic jaw movement ends this problem of dose penumbra above and below the target. The RSS delivery produces highly improved longitudinal dose conformity, leaving only some unavoidable low dose outside the field due to electron transport and photon scatter. The primary beam does not irradiate the tissue before and after the tumor. The time required for an RSS fraction is similar to that for a regular delivery fraction with the corresponding field width. However, now the use of the 5-cm-field width becomes clinically feasible since the drawbacks of extensive dose exposure to healthy tissue above and below the target volume are abandoned. The use of the 5-cm fan beam reduces the beam-on time compared to a plan with similar parameters, theoretically by 50%. In this planning study, the mean radiation time of RSS 5 was 58% compared to that of RSS 2.5. At the same time, mean and maximum doses to the optic pathways are reduced significantly.

The dynamic jaws allow an additional improvement of longitudinal dose conformity within the target volume by

Table 3. Ten different patient plans in five different delivery modes*

Plan	Parameter	REG 2.5	REG 5	RSS 2.5	RSS 5	DJDC 5
Boost PT	D_{99}	64.9 ± 2.0	62.7 ± 1.7	65.7 ± 1.7	64.2 ± 2.4	64.5 ± 1.6
	Mean	70.0 ± 0.2	69.6 ± 0.1	70.4 ± 0.1	70.3 ± 0.1	70.2 ± 0.1
	SD	1.64 ± 0.43	2.28 ± 0.49	1.44 ± 0.30	1.88 ± 0.46	2.06 ± 0.44
	D_1	72.9 ± 0.6	73.5 ± 0.7	73.5 ± 0.7	74.2 ± 0.9	73.1 ± 1.1
	CI_{95}	1.11 ± 0.05	1.11 ± 0.05	1.29 ± 0.09	1.35 ± 0.08	1.34 ± 0.06
	UI	1.08 ± 0.02	1.11 ± 0.03	1.06 ± 0.01	1.09 ± 0.02	1.09 ± 0.02
	$V_{95\%}$	0.950 ± 0.041	0.882 ± 0.046	0.982 ± 0.013	0.966 ± 0.019	0.962 ± 0.025
	$V_{105\%}$	0.003 ± 0.004	0.009 ± 0.011	0.007 ± 0.007	0.019 ± 0.013	0.023 ± 0.019
Boost ln	D_{99}	65.0 ± 2.0	63.6 ± 2.0	68.0 ± 0.7	67.1 ± 1.3	66.9 ± 1.7
	Mean	70.0 ± 0.2	69.5 ± 0.6	70.3 ± 0.2	70.2 ± 0.2	70.2 ± 0.4
	SD	1.62 ± 0.34	2.03 ± 0.42	0.98 ± 0.33	1.25 ± 0.40	1.58 ± 0.59
	D_1	73.0 ± 0.8	73.3 ± 0.9	73.0 ± 1.2	73.2 ± 1.0	73.6 ± 1.4
	CI_{95}	1.11 ± 0.05	1.12 ± 0.05	1.29 ± 0.09	1.35 ± 0.09	1.34 ± 0.06
	UI	1.08 ± 0.02	1.10 ± 0.02	1.04 ± 0.02	1.06 ± 0.02	1.07 ± 0.02
	$V_{95\%}$	0.958 ± 0.033	0.894 ± 0.062	0.997 ± 0.003	0.989 ± 0.01	0.983 ± 0.01
	$V_{105\%}$	0.004 ± 0.005	0.009 ± 0.012	0.005 ± 0.008	0.007 ± 0.008	0.018 ± 0.019
PTV nodes	D_{99}	52.2 ± 2.4	51.9 ± 2.2	53.2 ± 1.2	52.4 ± 1.5	52.2 ± 1.8
	Mean	58.4 ± 0.2	58.8 ± 0.7	59.4 ± 0.4	59.7 ± 0.5	59.4 ± 0.6
	SD	3.0 ± 0.4	3.2 ± 0.5	3.7 ± 0.3	3.9 ± 0.4	4.0 ± 0.6
	D_1	68.2 ± 0.7	68.1 ± 0.9	69.8 ± 0.5	70.5 ± 0.7	70.4 ± 0.8
	CI_{95}	1.25 ± 0.08	1.28 ± 0.10	1.25 ± 0.04	1.32 ± 0.03	1.31 ± 0.03
	UI	1.18 ± 0.02	1.19 ± 0.03	1.21 ± 0.01	1.22 ± 0.02	1.23 ± 0.02
	$V_{95\%}$	0.966 ± 0.024	0.948 ± 0.037	0.979 ± 0.008	0.971 ± 0.014	0.962 ± 0.022
	$V_{105\%}$	0.156 ± 0.029	0.222 ± 0.071	0.252 ± 0.051	0.293 ± 0.054	0.288 ± 0.057
Parotids	Mean	24.8 ± 2.3	26.0 ± 2.3	25.2 ± 2.8	26.1 ± 2.5	26.0 ± 1.4
Optic nerves	Max	50.9 ± 3.7	52.3 ± 0.9	46.4 ± 11.2	47.1 ± 10.3	46.9 ± 10.5
	Mean	34.5 ± 4.2	41.4 ± 2.2	24.7 ± 8.6	27.0 ± 8.7	28.0 ± 9.3
Chiasm	Max	49.1 ± 5.2	51.7 ± 1.2	30.7 ± 17.9	32.5 ± 18.3	31.8 ± 17.4
	Mean	39.5 ± 7.1	46.8 ± 2.0	19.5 ± 12.9	21.0 ± 13.5	21.3 ± 14.1
Brain (ml)	V_{10} Gy	317 ± 81	458 ± 57	243 ± 72	267 ± 71	277 ± 69
	V_{30} Gy	66 ± 19	112 ± 24	66 ± 21	83 ± 19	84 ± 22
	V_{60} Gy	3 ± 3	4 ± 3	4 ± 3	6 ± 4	7 ± 3
Lung apex (ml)	V_{10} Gy	135 ± 75	190 ± 81	109 ± 82	111 ± 80	121 ± 94
	V_{30} Gy	26 ± 11	41 ± 15	33 ± 17	35 ± 16	35 ± 18
	V_{50} Gy	1 ± 1	2 ± 2	3 ± 2	4 ± 3	6 ± 3
Integral dose (Gy x l)		256.7 ± 42.0	288.7 ± 54.9	233.6 ± 43.8	242.0 ± 44.0	240.5 ± 40.8
Radiation time (sec)		595 ± 89	319 ± 35	570 ± 98	333 ± 58	199 ± 19

Abbreviations: CI_{95} = 95% isodose conformity index; UI = uniformity index; REG = regular delivery; RSS = running-start-stop delivery; DJDC = dynamic jaw dynamic couch delivery; REG 2.5 or REG 5 = field width; Boost ln = boost lymph node.

* Table shows mean values of 10 different patient plans in five different delivery modes and parameter settings displayed in Gy ± standard deviations (SD)

adapting the optimal fan beam width to the specific area of the target. Flexible use of intensity modulation in combination with flexible field width can optimize dose gradients; therefore, regions of complex geometry like the skull base or the parotid area can be treated with a smaller field width, while the cervical nodes inferior to that region require lower-intensity modulation and customized dose gradients and can be treated with the biggest possible field width. With the addition of dynamic couch movement, the radiation time can be reduced even further, resulting in a mean calculated beam-on time of 199 sec. The flexible use of couch speed results in additional customized intensity modulation, thereby allowing the intensity modulation factor generated by the leaves to be lower. The beam-on time is proportional to the modulation factor, so using the couch speed to achieve modulation provides an additional speed improvement.

Overcoming the problems of dose penumbra above and below the target might potentially be beneficial in terms of secondary malignancy induction. The unique characteristic of low-dose spillage present in IMRT in general and the possible consequences of increased secondary tumor induction have been widely discussed (24, 25). The new technology presented here does not change the way the dose is applied over 360° and therefore does not change this fact; however, it does minimize dose exposure to healthy tissue above and below the target, so it reduces at least part of this potentially increased risk. This can be especially important for young patients with high susceptibility to secondary malignancies (children in general and Hodgkin's lymphoma patients). The gain from this reduced dose exposure will be of special interest when small volumes are treated. Here, the relative volume of unnecessarily irradiated healthy tissue is even

more important, *e.g.*, in small benign lesions. For the same reasons, radiosurgical treatments or small volume reirradiations with dose gradients steeper than previously treated areas are indications with a high potential for this technique.

Similar to flexible use of the jaws, couch speed can now be varied in different areas. The combination of all dynamic components allows reduction of the beam-on time of the best currently available plan with 2.5 cm of 595 sec, on average, by 67%, to now 199 sec on average. This time gain can be even higher in multitarget treatments, since the travel distance itself between separated lesions can be covered with maximal couch speed of 10 cm/sec and is not determined by the couch speed used within a target volume. In addition to these maximized movement options, rotational beam delivery with a static couch will also be possible. This might be beneficial for tumors smaller than the maximal field width, *e.g.*, radiosurgical cases of brain metastases or arteriovenous malformations.

The speed of IMRT delivery is a topic highly discussed in the current literature. In times of financial crisis and budget cuts in many parts of the world, the economic pressure on many departments increases, and high patient throughput is a high priority. In addition, many new solutions to fast single-arc IMRT are presented, and many older ones have been revitalized (26). This new form of helical tomotherapy delivery will add more aspects to this heated debate.

However, it is important to note that the data presented here represent the future of helical tomotherapy delivery, and it is not possible to deliver these plans without some minor modifications to the present machines and the currently available software. In addition, the time gain of 67% stated above reflects improvements to the beam-on time only. Therefore, patient load will not be increased by 67%, since the required time for immobilization, megavoltage CT acquisition, and registration process remains unchanged.

CONCLUSIONS

The current delivery mode of helical tomotherapy produces excellent dose distributions for complex and challenging cases of locally advanced nasopharyngeal cancer. The new technology of dynamic jaw and couch movements improves the longitudinal dose conformity and cuts off the previously unavoidable dose penumbra superiorly and inferiorly to the target. It thereby reduces integral dose and provides better treatment options when steep craniocaudal dose gradients are needed. It facilitates the use of the largest field width for faster treatments. The combination of dynamic jaw and couch movements reduces the beam-on time and allows an accelerated treatment especially of big or multiple targets. The decreased radiation time increases patient comfort, minimizes potential problems of intrafractional motion, and can increase patient throughput.

REFERENCES

1. Mackie TR, Balog J, Ruchala K, *et al*. Tomotherapy. *Semin Radiat Oncol* 1999;9:108–117.
2. Welsh JS, Patel RR, Ritter MA, *et al*. Helical tomotherapy: An innovative technology and approach to radiation therapy. *Technol Cancer Res Treat* 2002;1:311–316.
3. Jeraj R, Mackie TR, Balog J, *et al*. Radiation characteristics of helical tomotherapy. *Med Phys* 2004;31:396–404.
4. Sterzing F, Schubert K, Sroka-Perez G, *et al*. Helical tomotherapy: Experiences of the first 150 patients in Heidelberg. *Strahlenther Onkol* 2008;184:8–14.
5. Rochet N, Sterzing F, Jensen A, *et al*. Helical tomotherapy as a new treatment technique for whole abdominal irradiation. *Strahlenther Onkol* 2008;184:145–149.
6. Sterzing F, Sroka-Perez G, Schubert K, *et al*. Evaluating target coverage and normal tissue sparing in the adjuvant radiotherapy of malignant pleural mesothelioma: Helical tomotherapy compared with step-and-shoot IMRT. *Radiother Oncol* 2008;86: 251–257.
7. Penagaricano JA, Papanikolaou N, Yan Y, *et al*. Feasibility of cranio-spinal axis radiation with the Hi-Art tomotherapy system. *Radiother Oncol* 2005;76:72–78.
8. Wong JY, Liu A, Schultheiss T, *et al*. Targeted total marrow irradiation using three-dimensional image-guided tomographic intensity-modulated radiation therapy: An alternative to standard total body irradiation. *Biol Blood Marrow Transplant* 2006;12:306–315.
9. Sterzing F, Welzel T, Sroka-Perez G, *et al*. Reirradiation of multiple brain metastases with helical tomotherapy: A multifocal simultaneous integrated boost for eight or more lesions. *Strahlenther Onkol* 2009;185:89–93.
10. Sheng K, Molloy JA, Read PW. Intensity-modulated radiation therapy (IMRT) dosimetry of the head and neck: A comparison of treatment plans using linear accelerator-based IMRT and helical tomotherapy. *Int J Radiat Oncol Biol Phys* 2006;65: 917–923.
11. Widesott L, Pierelli A, Fiorino C, *et al*. Intensity-modulated proton therapy versus helical tomotherapy in nasopharynx cancer: Planning comparison and NTCP evaluation. *Int J Radiat Oncol Biol Phys* 2008;72:589–596.
12. Lee N, Xia P, Fischbein NJ, *et al*. Intensity-modulated radiation therapy for head-and-neck cancer: The UCSF experience focusing on target volume delineation. *Int J Radiat Oncol Biol Phys* 2003;57:49–60.
13. Gregoire V, De Neve W, Eisbruch A, *et al*. Intensity-modulated radiation therapy for head and neck carcinoma. *Oncologist* 2007;12:555–564.
14. Fiorino C, Dell'Oca I, Pierelli A, *et al*. Simultaneous integrated boost (SIB) for nasopharynx cancer with helical tomotherapy. A planning study. *Strahlenther Onkol* 2007;183:497–505.
15. Kissick MW, Flynn RT, Westerly DC, *et al*. On the making of sharp longitudinal dose profiles with helical tomotherapy. *Phys Med Biol* 2007;52:6497–6510.
16. Mackie TR, Holmes T, Swerdloff S, *et al*. Tomotherapy: a new concept for the delivery of dynamic conformal radiotherapy. *Med Phys* 1993;20:1709–1719.
17. Yang JN, Mackie TR, Reckwerdt P, *et al*. An investigation of tomotherapy beam delivery. *Med Phys* 1997;24:425–436.
18. Eisbruch A, Foote RL, O'Sullivan B, *et al*. Intensity-modulated radiation therapy for head and neck cancer: emphasis on the selection and delineation of the targets. *Semin Radiat Oncol* 2002; 12:238–249.
19. Gregoire V, Eisbruch A, Hamoir M, *et al*. Proposal for the delineation of the nodal CTV in the node-positive and the post-operative neck. *Radiother Oncol* 2006;79:15–20.
20. Cannon DM, Lee NY. Recurrence in region of spared parotid gland after definitive intensity-modulated radiotherapy

for head and neck cancer. *Int J Radiat Oncol Biol Phys* 2007.
21. Kissick MW, Fenwick J, James JA, *et al*. The helical tomotherapy thread effect. *Med Phys* 2005;32:1414–1423.
22. Pirzkall A, Carol M, Lohr F, *et al*. Comparison of intensity-modulated radiotherapy with conventional conformal radiotherapy for complex-shaped tumors. *Int J Radiat Oncol Biol Phys* 2000;48:1371–1380.
23. Wolden SL, Chen WC, Pfister DG, *et al*. Intensity-modulated radiation therapy (IMRT) for nasopharynx cancer: Update of the Memorial Sloan-Kettering experience. *Int J Radiat Oncol Biol Phys* 2006;64:57–62.
24. Hall EJ, Wuu CS. Radiation-induced second cancers: The impact of 3D-CRT and IMRT. *Int J Radiat Oncol Biol Phys* 2003;56:83–88.
25. Kry SF, Salehpour M, Followill DS, *et al*. The calculated risk of fatal secondary malignancies from intensity-modulated radiation therapy. *Int J Radiat Oncol Biol Phys* 2005;62:1195–1203.
26. Bortfeld T, Webb S. Single-arc IMRT? *Phys Med Biol* 2009;54: N9–N20.